Effects of UV light intensity on electrochemical wet etching of SiC for the fabrication of suspended graphene

Ryong-Sok O[1-2*], Makoto Takamura[1], Kazuaki Furukawa[1], Masao Nagase[2], and Hiroki Hibino[1]

[1] NTT Basic Research Laboratories, Nippon Telegraph and Telephone Corporation, 3-1 Morinosato-Wakamiya, Atsugi, Kanagawa 243-0198, Japan

[2] Graduate School of Advanced Technology and Science, University of Tokushima, 2-1 Minami-josanjima, Tokushima 770-8506, Japan

***E-mail:** oryonsoku@ee.tokushima-u.ac.jp

Abstract

We report on the effects of UV light intensity on the photo assisted electrochemical wet etching of SiC (0001) underneath an epitaxially grown graphene for the fabrication of suspended structures. The maximum etching rate of SiC (0001) was 2.5 μm/h under UV light irradiation in 1 wt% KOH at a constant current of 0.5 mA/cm^2. The successful formation of suspended structures depended on the etching rate of SiC. In the Raman spectra of the suspended structures, we did not observe a significant increase in the intensity of the D peak, which originates from defects in graphene sheets. This is most likely explained by the high quality of the single-crystalline graphene epitaxially grown on SiC.

1. Introduction

The unique properties of graphene have attracted tremendous interest. Its intrinsic mechanical, electronic, and optical properties have been studied extensively using suspended graphene structures fabricated from exfoliated graphene flakes.[1–6] The mechanical exfoliation transfer method easily yields high quality graphene, but it is difficult to control the thickness and size of the flakes. On the other hand, the epitaxial growth of graphene by the thermal decomposition of a SiC (0001) substrate under vacuum or Ar ambient provides thickness-controlled single-crystalline graphene on a wafer scale.[7, 8] It is expected that a suspended graphene array can be fabricated on SiC substrates by combining photolithographic processes and the selective wet etching of SiC underneath the epitaxially grown graphene. Unfortunately, selective etching methods for fabricating suspended graphene structures on SiC substrates are limited because the SiC crystal is stable in the presence of most chemicals. For this reason, photo assisted electrochemical wet etching with aqueous KOH[9] has been used for selective etching to fabricate suspended graphene structures on SiC substrates[10–12].

The optimum conditions for the selective wet etching of SiC underneath the epitaxially grown graphene, however, have not been thoroughly investigated. Although UV light is used to improve the rate of photo assisted electrochemical wet etching[9–12], the defect formation in graphene sheets induced by UV light irradiation under various ambient conditions has also been reported[13–18]. Clarifying the quantitative effects of UV light irradiation on the etching rate of SiC and the defect formation in graphene sheets is important for the efficient fabrication of high-quality single-crystalline suspended graphene structures.

In this study, we investigated the effects of UV light on the selective wet etching of

SiC (0001) underneath the epitaxially grown graphene for the fabrication of suspended graphene structures. We investigated the relationship between the etching rate of SiC and UV light intensity, and evaluated the quality of suspended graphene using microscopic Raman spectroscopy. On the basis of the experimental results, we discuss the optimum conditions of selective wet etching for the fabrication of suspended graphene on SiC.

2. Experimental procedure

Figures 1(a)─1(d) illustrate the sample fabrication process. Graphene was grown epitaxially on 4H-SiC n-type (0001) substrates by heating the substrates in a 100 Torr Ar atmosphere at 1750 °C. The graphene comprises a monolayer and a bilayer at a ratio of about 1:1, as confirmed by atomic force microscopy (AFM, Bruker Multimode AFM) phase images and microscopic Raman spectroscopy (Renishaw in-Via Reflex) at the excitation wavelength λ = 532 nm. Suspended structures were fabricated as follows: First, epitaxially grown graphene layers [Fig. 1(a)] were patterned using photolithographic processes followed by oxygen plasma etching [Fig. 1(b)]. Next, Au/Ti layers (200 nm/5 nm), which formed the conductive electrodes and masking patterns that would work as clamps for the suspended graphene, were fabricated by electron beam evaporation and a lift-off process [Fig. 1(c)]. Then, each patterned graphene sample was placed in a quartz cell filled with aqueous KOH (1 wt%). The SiC substrate was etched at a constant current under focused UV irradiation for 3 h [Fig. 1(d)].

Figure 2(a) shows a diagram of the electrochemical wet etching apparatus. The SiC substrate with the patterned graphene sample was used as the anode. A Pt wire and Ag/AgCl (3M NaCl) were employed as the cathode and reference electrode, respectively. The voltage between the anode and the cathode was controlled with a

potentiostat in the constant current mode (0.5 mA/cm^2). During the wet etching process, the output voltage of the potentiostat was approximately 0.1 V. A 6 × 3.3 mm^2 area of the sample surface was patterned, as shown in Fig. 2(b). The graphene beams were patterned into a bow-tie shape (length and width of 10 and 4 μm, respectively) to prevent beam edge bending[14]. The patterned area, which contained 22 × 5 subareas, each of which possesses ten arrayed beams, was irradiated by UV light through an optical fiber using Xe light source. A large Au/Ti pad was used for a good electric contact to n-type SiC in the electrochemical wet etching process. The UV light intensity at the sample position was measured along the horizontal centerline of the focal plane using a photodetector. From the relationship between the UV light intensity and the distance from the focus, it was estimated that the UV light intensity was distributed concentrically, as shown in Fig. 2(c). After the wet etching process, the etch depth of SiC at each subarea, shown in Fig. 2(b), was measured with a profilometer. The suspended structure fabricated by the wet etching process was characterized by scanning electron microscopy (SEM, Zeiss Ultra 55).

3. Results and discussion

3.1 Effect of UV light on epitaxially grown graphene on SiC

We investigated the effect of UV light irradiation on the epitaxially grown graphene immersed in aqueous KOH (1 wt%) in the absence of a constant current. Figure 3 shows Raman spectra of a sample before and after UV light irradiation for 3 h. We measured the Raman spectra of the epitaxially grown graphene after UV light irradiation at the focal point where the intensity was maximum (about 50 mW/cm^2) and subtracted the SiC-related background in the spectra.[19–22] No significant change in D peak intensity (~1350 cm^{-1}), which originates from defects in graphene sheets,[10–18, 23, 24] was observed.

Thus, we confirmed that no defects were formed in the epitaxially grown graphene on SiC immersed in aqueous KOH (1 wt%) upon irradiation with strong UV light.

In earlier studies, defect formation in graphene sheets under UV light irradiation was induced by the reactive species generated by photo dissociation reactions of ambient gases[13–17]. Our experimental results suggest that the reactive species that induce defect formation in graphene sheets were not generated in the aqueous KOH (1 wt%) under UV light irradiation. On the other hand, photo induced defect formation by the UV light irradiation of chemical vapor deposition (CVD)-grown graphene in vacuum has been reported[17–18]. However, it was pointed out that defect sites such as grain boundaries in CVD-grown graphene[24, 25] and ripples or corrugations in the graphene might be damaged intensively by UV light irradiation[17, 18]. In addition, it was reported that defect formation in graphene under UV light irradiation strongly depends on the interaction between the graphene and the substrate[18]. Our experimental results also suggest that the condition of the epitaxially grown graphene on SiC is sufficiently optimized to prevent photo induced defect formation under UV light irradiation.

3.2 Effect of UV light intensity on the etching rate of SiC underneath epitaxially grown graphene

We discuss the quantitative dependence of the etching rate of SiC on the UV light intensity on the patterned area. The variation in the etching rate of SiC in the patterned area strongly correlated with the UV light intensity. Figure 4 shows a plot of the etching rate of SiC versus UV light intensity. In the low-intensity regime (< 20 mW/cm^2), the etching rate increased nonlinearly with UV light intensity until it reached 2.0 μm/h. To increase the etching rate of SiC, a UV light intensity of at least 5 mW/cm^2 was required. At higher UV light intensities, the etching rate saturated at 2.5 μm/h. These results can

be explained by the increase and the saturation of photo induced electron-hole pairs generated by UV light irradiation on the SiC substrate. Kato et al. have reported an etching rate of about 0.3 μm/h at a constant current of 5 mA/cm^2 when the SiC substrate was not irradiated by UV light[9]. However, in our case, the etching rate of the nonirradiated region was nearly zero. This suggests that the photo induced current dominated the etching reaction. Therefore, we consider the UV light intensity to be an important parameter in the photo assisted electrochemical wet etching of SiC.

In our experiment, suspended structures were successfully formed in subareas where the UV light intensity was 5–10 mW/cm^2, where the etching rate and depth near the suspended structures were 0.5–0.8 μm/h and 1.5–2.4 μm, respectively. On the other hand, in subareas where the UV light intensity was more than 10 mW/cm^2, all of the graphene beam structures collapsed. On the basis of the experimental results shown in Fig. 3, we can exclude photo induced defect formation under the UV light irradiation as the cause of the collapse. Thus, we consider that the collapse of the beam structures was caused mainly by the intrinsic strain in the metal film released by the undercutting of SiC underneath the metal film, pulling and tearing the graphene. The etching rate and depth near the collapsed structures were more than 0.8 μm/h and 2.4 μm, respectively. Under this high etching rate, the undercutting of SiC underneath the metal film progressed rapidly and led to the collapse of graphene beam structures. The etching rate and depth near the surviving structures varied with experimental conditions, but they were considered important criteria for determining the success or failure of the fabrication of suspended structures.

The etching selectivity of SiC for graphene is the most important factor in the fabrication of suspended structures. The minimum selectivity (SiC/graphene) estimated

from the maximum etch depth of SiC near the surviving beam structure (2.4 μm) and the thickness of bilayer graphene (0.335 × 2 nm) was approximately 3600. This large value (> 1000[26]) is promising as it indicates the successful fabrication of the suspended structures.

3.3 Characterization of suspended graphene fabricated by wet etching

Figure 5(a) shows an SEM image of a suspended structure after the wet etching of a subarea where the etch depth was approximately 1.5 μm. To characterize this structure, we compared microscopic Raman spectra of the structure before and after it was subjected to electrochemical wet etching, as shown in Fig. 5(b). After the wet etching process, the intensities of G and 2D peaks (at approximately 1600 and 2700 cm^{-1}, respectively), which originate from the sp^2 network of carbon atoms constituting the graphene sheets,[23] increased, whereas those of the SiC-related background (around 1519 and 1712 cm^{-1}) decreased. Since the SiC substrate underneath the epitaxially grown graphene was etched selectively (approximately 1.5 μm), the distance between the SiC substrate and the graphene was increased, reducing the intensities of the SiC-related background after the wet etching. This is consistent with the dependence of the intensities of the SiC-related background on the laser focus position of microscopic Raman spectroscopy in the depth direction[19]. The SiC-related background in Raman spectra was not completely eliminated after etching. This could be due to the insufficiently large distance between the suspended structure and the SiC substrate or the small amount of residual SiC remaining underneath the graphene layer. SEM observations enable us to check the extent of residual SiC. In our case, it was not evident whether residual SiC remained beneath the suspended structure. However, from Fig. 5(a), it seems that the amount of residual SiC, if any, would be small. Thus, the

effect of residual SiC on the suspended structure will be excluded from the following discussion. On the basis of the Raman spectra after the subtraction of the SiC-related background shown in Fig. 5(c), the increase in 2D peak full-width at half maximum (FWHM) from 48 to 62 cm^{-1} after wet etching suggests an increase in the dominant thickness of graphene from monolayer to bilayer[20] after wet etching. This indicates that the C-rich layer at the interface between SiC and the epitaxially grown graphene (buffer layer)[7, 8] was decoupled from the SiC and formed an additional layer of graphene.[13, 14] In the literature, etching-reaction-induced defect formation in graphene sheets has been reported.[10–12] In our case, the intensity of the D peak after wet etching was very low, as shown in Figs. 5(b) and 5(c). The graphene was not damaged during the wet etching process under UV light irradiation. We think that, this is most likely because the initial crystal quality of the graphene could be very high.

Raman spectra of the epitaxially grown graphene on SiC are known to be strongly modulated by the compressive strain in graphene[20–22]. This strain is caused by the difference in thermal expansion coefficient between graphene and SiC. In this case, the positions of G and 2D peaks are observed at higher wave numbers[20-22] than those of unstrained graphene.[23] After the graphene is decoupled from SiC by wet etching, the modulation effect of the Raman spectrum induced by compressive strain from SiC is eliminated. In practice, the positions of the G and 2D peaks after wet etching shifted from 1605 and 2709 cm^{-1} to 1577 and 2661 cm^{-1}, respectively. For the undoped and unstrained monolayer graphene supported by a substrate, G and 2D peaks have been observed at around 1585 and 2683 cm^{-1}, respectively.[23] From the difference in peak position between unstrained monolayer graphene and epitaxially grown graphene, we can estimate the compressive strain in a sample.[21, 22] Here, note that the G peak position

is sensitive to the variation in electron concentration in graphene[27] caused by electron doping from SiC.[7] Thus, the strain in the epitaxially grown graphene on SiC should be estimated from the shift of the 2D peak position. We estimated the compressive strain in monolayer graphene before wet etching to be about 0.37% from the upshift of the 2D peak position ($\Delta\omega_{2D\ before}$ = 2709 cm^{-1} − 2683 cm^{-1} = 26 cm^{-1}). Owing to the relaxation of compressive strain and an increase in the dominant thickness of graphene from monolayer to bilayer after wet etching[10–12], we expected G and 2D peaks to be observed at around 1580 and 2701 cm^{-1}, respectively.[12, 23] However, the peak positions were shifted considerably to a lower wave number than those of unstrained bilayer graphene. The differences in both the peak positions between the unstrained bilayer graphene[23] and the graphene structure after wet etching were $\Delta\omega_{G\ after}$ = 1577 cm^{-1} − 1580 cm^{-1} = −3 cm^{-1} and $\Delta\omega_{2D\ after}$ = 2661 cm^{-1} – 2701 cm^{-1} = −40 cm^{-1}, respectively. The downshift of the 2D peak after wet etching indicates a tensile strain of about 0.55% in the bilayer graphene. The causes of tensile strain in graphene may be the bending of the graphene beam[1] and the intrinsic strain in the metal film[28]. However, in our case, the G peak did not follow the downshift trend of the 2D peak and was not affected by tensile strain[28, 29]. Further investigations of the self-doping effect of the graphene beam[6] and the unintentional carrier doping effect of the photoresist residue[30] are required to clarify the causes of the downshift. We confirmed that the compressive strain in graphene induced by the SiC substrate was completely eliminated. This suggests that the SiC underneath the epitaxially grown graphene was etched selectively.

4. Conclusions

We investigated the effect of UV light intensity on the photo assisted electrochemical wet etching of SiC underneath an epitaxially grown graphene used for the fabrication of

suspended graphene structures. We measured the etching rate of SiC and UV light intensity on the sample using a profilometer and a photodetector, respectively. The etching rate of SiC was found to depend strongly on the UV light intensity. The etching rate in the nonirradiated region was nearly zero. The maximum etching rate of SiC was ~2.5 μm/h at a constant current density (0.5 mA/cm^2). The collapse of graphene structures was caused mainly by the undercutting of SiC underneath the metal film. The estimated minimum etching selectivity (SiC/graphene) was more than 3000. The photo induced defect formation in graphene was not observed either in the presence of the current or in its absence. These results suggest that controlling UV light intensity is essential for the highly reproducible fabrication of suspended graphene structures.

References

1) J. S. Bunch, A. M. van der Zande, S. S. Verbridge, I. W. Frank, D. M. Tanenbaum, J. M. Parpia, H. G. Craighead, and P. L. McEuen: Science **315**, 490 (2007).
2) C. Chen, S. Rosenblatt, K. I. Bolotin, W. Kalb, P. Kim, I. Kymissis, H. L. Stormer, T. F. Heinz, and J. Hone: Nat. Nanotechnol. **4**, 861 (2009).
3) V. Singh, S. Sengupta, H. S. Solanki, R. Dhall, A. Allain, S. Dhara, P. Pant, and M. M. Deshmukh: Nanotechnology **21**, 165204 (2010).
4) K. I. Bolotin, K. J. Sikes, Z. Jiang, M. Kilma, G. Fundenberg, J. Hone, P. Kim, and H. L. Stormer: Solid State Commun. **146**, 351 (2008).
5) K. I. Bolotin, K. J. Sikes, J. Hone, H. L. Stormer, and P. Kim: Phys. Rev. Lett. **101**, 096802 (2008).
6) S. Berciaud, S. Ryu, L. E. Brus, and T. F. Heinz : Nano Lett. **9**, 346 (2009).
7) K. V. Emtsev, A. Bostwick, K Horn, J. Jobst, G. L. Kellogg, L. Ley, J. L. McChesney, T. Ohta, S. A. Reshanov, J. Rohrl, E. Rotenberg, A. K. Schmid, D. Waldmann, H. B. Weber, and T. Seyller: Nat. Mater. **8**, 203 (2009).
8) H. Hibino, H. Kageshima, and M. Nagase: J. Phys. D: Appl. Phys. **43**, 374005 (2010).
9) M. Kato, M. Ichimura, E. Arai, and P. Ramasamy: Jpn. J. Appl. Phys. **42**, 4233 (2003).
10) S. Shivaraman, R. A. Barton, X. Yu, J. Alden, and L. Herman: Nano Lett. **9**, 3100 (2009).
11) S. Shivaraman, J. Jobst, D. Waldmann, H. B. Weber, and M. G. Spencer: Phys. Rev. B **87**, 195425 (2013).

12) M. Takamura, K. Furukawa, H. Okamoto, S. Tanabe, H. Yamaguchi, and H. Hibino: Jpn. J. Appl. Phys. **52**, 04CH01 (2013).

13) S. Huh, J. Park, Y. Kim, K. Kim, B. Hong, and J. Nam: ACS Nano **5**, 9799 (2011).

14) E. X. Zhang, A. K. M. Newaz, B. Wang, C. X. Zhang, D. M. Fleetwood, K. I. Bolotin, R. D. Schrimpf, S. T. Pantelides, and M. L. Alles: Appl. Phys. Lett. **101**, 121601 (2012).

15) S. Zhao, S. P. Surwade, Z. Li, and H. Liu: Nanotechnology **23**, 355703 (2012).

16) F. Gunes, G. Han, H. Shin, S. Lee, M. Jin, D. Duong, S. Chae, E. Kim, F. Yao, A. Benayad, J. Choi, and Y. Lee: NANO **6**, 409 (2011).

17) G. Imamura and K. Saiki: Chem. Phys. Lett. **587**, 56 (2013).

18) G. Imamura and K. Saiki: J. Phys. Chem. C **118**, 11842 (2014).

19) J. Kunc, Y. Hu, J. Palmer, C. Berger, and W. A. de Heer: Appl. Phys. Lett. **103**, 201911 (2013).

20) D. S. Lee, C. Riedl, B. Krauss, K. von Klitzing, U. Strake, and J. H. Smet: Nano Lett. **8**, 4320 (2008).

21) N. Ferralis, R. Maboundian, and C. Carraro: Phys. Rev. Lett. **101**, 156801 (2008).

22) R. O, A. Iwamoto, Y. Nishi, Y. Funase, T. Yuasa, T. Tomita, M. Nagase, H. Hibino, and H. Yamaguchi: Jpn. J. Appl. Phys. **51**, 06FD06 (2012).

23) A. C. Ferrari: Solid State Commun. **143**, 47 (2007).

24) Q Yu, L. A. Jauregui, W. Wu, R. Colby, J. Tian, Z. Su, H. Cao, Z. Liu, D. Pandey, D. Wei, T. F. Chung, P. Peng, N. P. Buisinger, E. A. Stach, J. Bao, S. S. Pei, and Y. P. Chen: Nat. Mater. **10**, 443 (2011).

25) X. Li, W. Cai, J. An, S. Kim, J. Nah, D. Yang, R. Piner, A. Velamakanni, I. Jung, E. Tutuc, S. K. Banerjee, L. Colombo, and R. S. Ruoff: Science **324**, 1312 (2009).

26) F. Chien, C. Wu, Y. Chou, T. Chen, S. Gwo, and W. Hsieh: Appl. Phys. Lett. **75**, 242 (1999).

27) A. Das, S. Pisana, B. Chakraborty, S. Piscanec, S. K. Saha, U. V. Waghmare, K. S. Novoselov, H. R. Krishnamurthy, A. K. Geim, A. C. Ferrari, and A. K. Sood: Nat. Nanotechnol. **3**, 210 (2008).

28) H. Shioya, M. Craciun, S. Russo, M. Yamamoto, and S. Tarucha: Nano Lett. **14**, 1158 (2014).

29) T. M. G. Mohiuddin, A. Lombardo, R. R. Nair, A. Bonetti, G. Savini, R. Jalil, N. Bonini, D. M. Basko, C. Galiotis, N. Marzari, K. S. Novoselov, A. K. Geim, and A. C. Ferrari: Phys. Rev. B **79**, 205433 (2009).

30) X. Dong, D. Fu, W. Fang, Y. Shi, P Chen, and L. Li: Small **5**, 1422 (2009).

Figure captions

Fig. 1. Illustration of the sample fabrication process: (a) Graphene was grown epitaxially on 4H-SiC n-type (0001) substrates. (b) The graphene beam structure was fabricated via the combination of a lithographic process and oxygen plasma etching. (c) Au/Ti layers (200 nm/5 nm) for conductive electrodes and masking patterns of the clamping for the beam structures were fabricated by electron beam evaporation and a lift-off process. (d) The SiC substrate was selectively etched in a quartz cell filled with dilute KOH (1 wt%) under a constant current and a focused UV irradiation.

Fig. 2. Illustration of the photo assisted electrochemical wet etching process: (a) Schematic of the wet etching apparatus. (b) Top view of sample after the fabrication of Au/Ti layers. The 6 × 3.3 mm^2 area of the sample enclosed by a red-dashed line was patterned. The area contains 22 × 5 subareas, each of which possesses ten arrayed beams. The length and width of graphene beams were 10 and 4 μm, respectively. (c) Relationship between the UV light intensity at λ = 300 nm and distance from the UV light focal point in horizontal direction. From this relationship, the UV light intensity over the patterned area was determined to be distributed concentrically.

Fig. 3. Raman spectra of epitaxial graphene grown on SiC immersed in dilute KOH (1 wt%) before and after UV light irradiation for 3 h in the absence of a constant current. SiC-related peaks in each spectrum were subtracted.

Fig. 4. Plot of etching rate of SiC versus UV light intensity for each subarea in the patterned area.

Fig. 5. Suspended structure obtained by electrochemical wet etching. (a) SEM image of the suspended structure. (b) Comparison of the raw Raman spectra of pristine epitaxial graphene and suspended structure. (c) Raman spectra after the subtraction of the SiC-related background. The spectrum measured on the graphene on SiC was magnified four times.

Figures

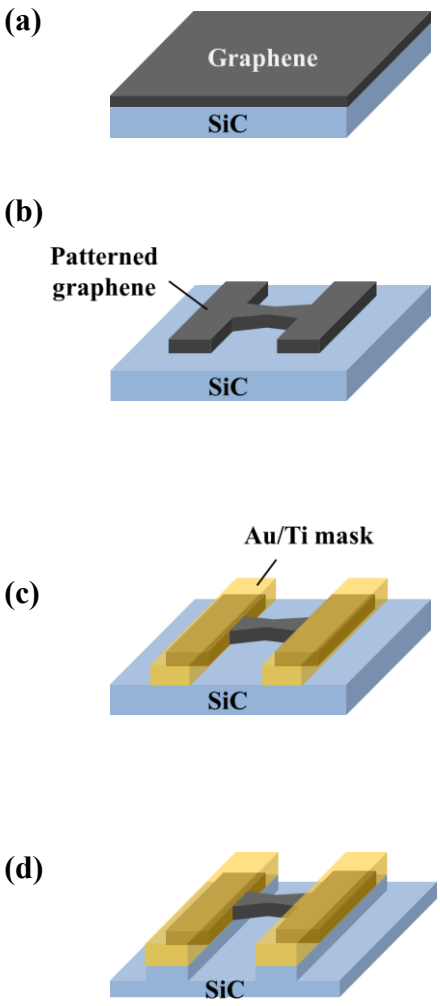

Fig. 1 (Color online)

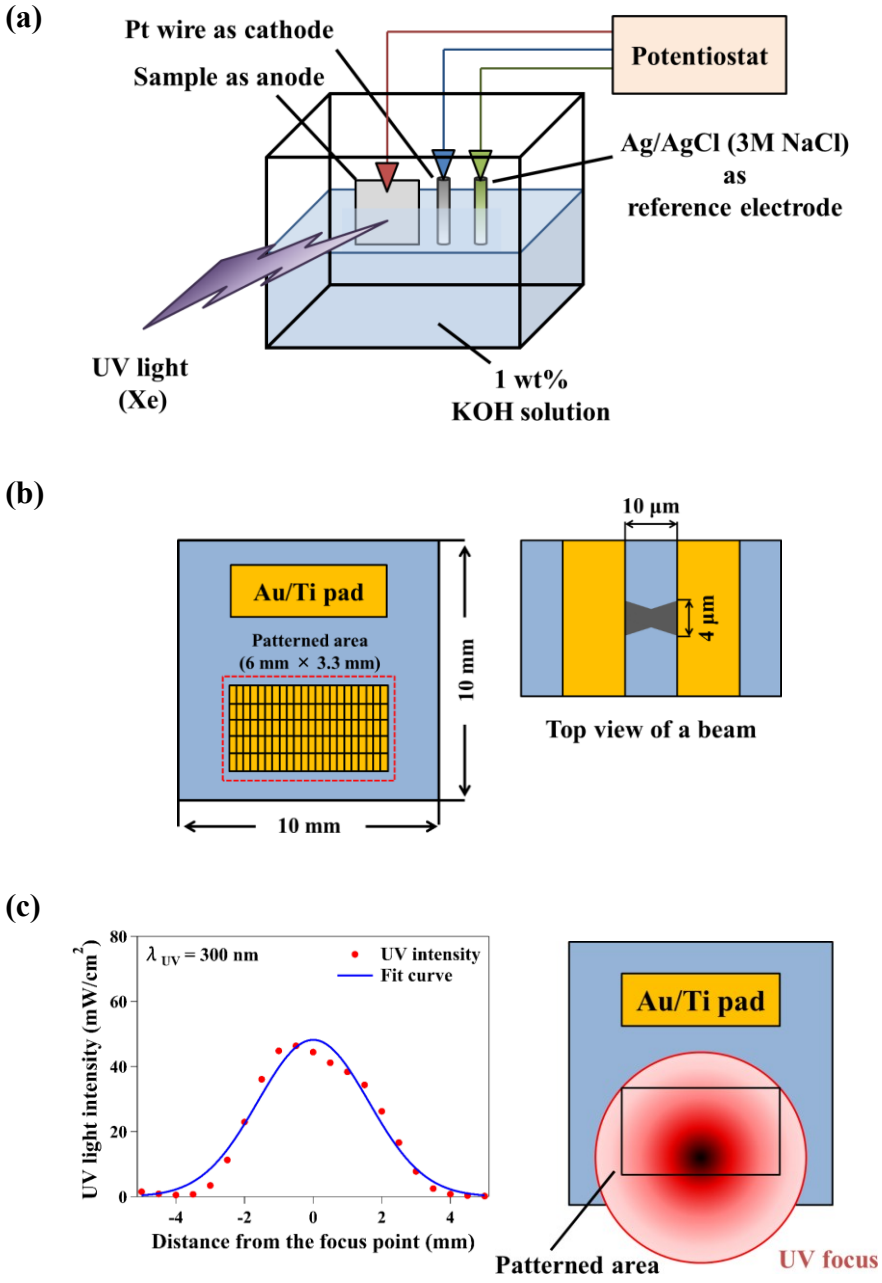

Fig. 2 (Color online)

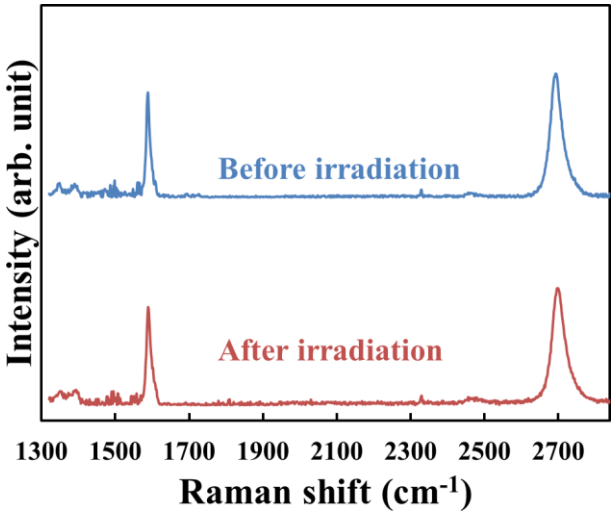
Intensity (arb. unit)
Before irradiation
After irradiation
1300
1500
1700
1900
2100
2300
2500
2700
Raman shift (cm-1)

Fig. 3

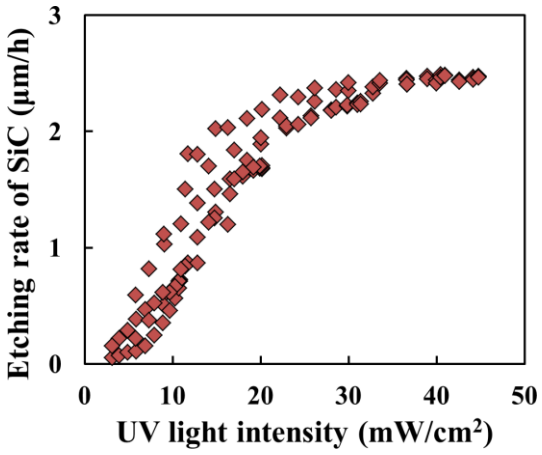
Etching rate of SiC (μm/h)
0
1
2
3
0
10
20
30
40
50
UV light intensity (mW/cm²)

Fig. 4

(a)

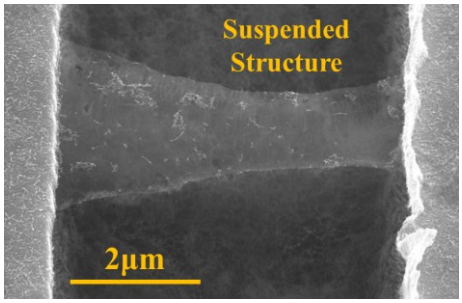

(b)

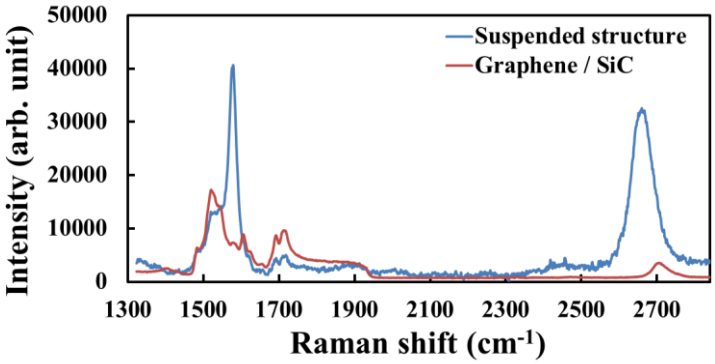

(c)

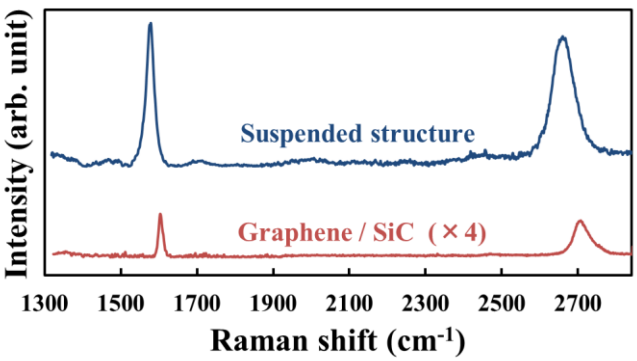

Fig. 5 (Color online)